

Differentiable Particles for General-Purpose Deformable Object Manipulation

Siwei Chen, Yiqing Xu, Cunjun Yu, Linfeng Li and David Hsu

National University of Singapore

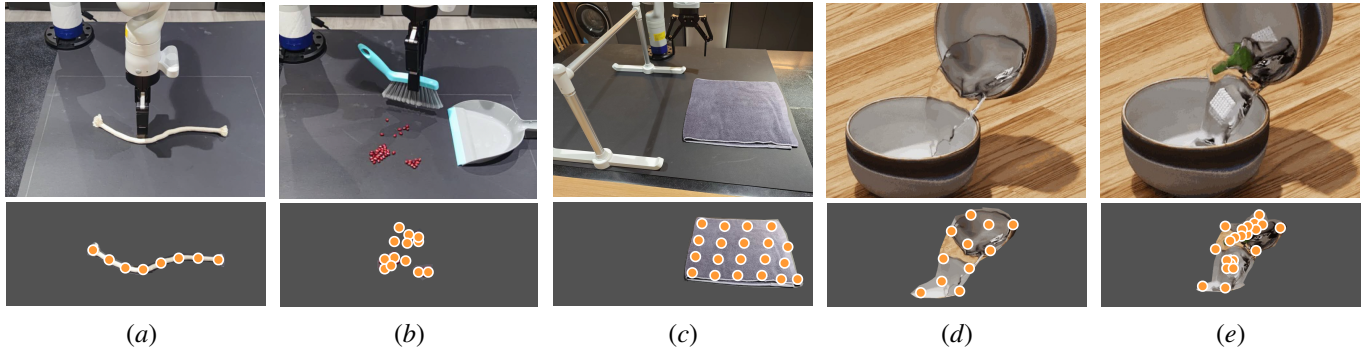


Fig. 1: Deformable object manipulation tasks used in evaluation: the first three on a real robot and the last two in simulation. (a) Straighten the rope via pushing. (b) Sweep the scattered beans into a tray. (c) Hang a piece of cloth on a rack. (d) Pour liquid into a bowl. (e) Pour soup, a liquid-solid mixture, into a bowl. The top row shows the robot in action. The bottom row shows the corresponding particle representations.

Abstract—Deformable object manipulation is a long-standing challenge in robotics. While existing approaches often focus narrowly on a specific type of object, we seek a general-purpose algorithm, capable of manipulating many different types of objects: beans, rope, cloth, liquid, One key difficulty is a suitable representation, rich enough to capture object shape, dynamics for manipulation and yet simple enough to be acquired effectively from sensor data. Specifically, we propose *Differentiable Particles* (DiPac), a new algorithm for deformable object manipulation. DiPac represents a deformable object as a set of *particles* and uses a *differentiable* particle dynamics simulator to reason about robot manipulation. To find the best manipulation action, DiPac combines learning, planning, and trajectory optimization through differentiable trajectory tree optimization. Differentiable dynamics provides significant benefits and enable DiPac to (i) estimate the dynamics parameters efficiently, thereby narrowing the sim-to-real gap, and (ii) choose the best action by backpropagating the gradient along sampled trajectories. Both simulation and real-robot experiments show promising results. DiPac handles a variety of object types. By combining planning and learning, DiPac outperforms both pure model-based planning methods and pure data-driven learning methods. In addition, DiPac is robust and adapts to changes in dynamics, thereby enabling the transfer of an expert policy from one object to another with different physical properties, e.g., from a rigid rod to a deformable rope.

I. INTRODUCTION

Deformable object manipulation (DOM) is a long-standing challenge in robotics, because it involves a large degree of freedom and complex non-linear dynamics. Existing approaches often focus narrowly on a specific type of objects: rope [37, 23, 27], cloth [10, 7, 21, 25], liquid [32, 41, 19],

. . . . Such a strategy is unlikely to exhaust the wide variety of different deformable objects. It is essential to develop a *general-purpose* DOM algorithm that handles many different types of objects uniformly. Our work is a step in this direction.

One key difficulty is a suitable representation, which is rich enough to capture the complex object shape, object dynamics for manipulation and yet simple enough to be acquired effectively from sensor data. We represent a deformable object as a set of *particles*, i.e., 3-D points with associated physical properties, and use a differentiable particle dynamics simulator to approximate object dynamics.

The particle representation provides multiple benefits. First, it is general and capable of representing a wide variety of objects: 0-dimensional beans, 1-dimensional rope, 2-dimensional cloth, and 3-dimensional liquid (Fig. 1). Further, differentiable particle dynamics enables efficient gradient-based optimization. Finally, particle dynamics is computationally efficient with parallel implementation on modern GPUs.

Our new algorithm, *Differentiable Particles* (DiPac), takes RGBD images of a deformable object as input and outputs a sequence of robot manipulation actions, until a specified goal is reached. To find the best action, DiPac combines three elements—learning, planning, and trajectory optimization—through differentiable trajectory tree optimization. It adopts an uncommon policy representation for manipulation: a computational graph consisting of a trajectory tree parameterized by the differentiable particle-based dynamics simulation model. The entire computational graph is end-to-end differentiable

for both model calibration and action selection. During the offline model calibration phase, the robot learns the dynamics parameters of the simulator by interacting with the real object.

It is important to note that the key objective of our model calibration is to enhance the model prediction accuracy for action selection rather than to uncover the ground-truth physics. During the online action selection phase, DiPac uses the calibrated dynamics simulator to reason about manipulation actions. Guided by a learned initial policy, it searches the trajectory tree for the best actions. In both phases, differentiability plays a critical role and allows DiPac to update the dynamics parameters and find the best actions through backward gradient propagation.

The policy representation of DiPac is aligned in spirit with the *Differentiable Algorithm Network* (DAN) framework [16]. The gist of DAN is to represent a robot control policy as a model and an associated algorithm that solves the model, both encoded together in a neural network (NN). The NN policy representation is fully differentiable and can be trained end-to-end from data. DiPac uses a particle dynamics simulator as the model and a trajectory tree optimizer as the algorithm. While it does not use a NN for policy representation, the trajectory tree plays the same role and is fully differentiable.

We evaluated DiPac on tasks on several distinct DOM tasks: straightening a rope via pushing, sweeping scattered beans into a target region, hanging a towel on a rack, and pouring liquid or soup. While specialized methods may perform better on any particular one of these tasks, DiPac performs capably over all of them. Furthermore, by combining planning and learning, DiPac outperforms both pure model-based planning methods and pure data-driven learning methods, including two state-of-the-art methods, Diffusion Policy [6] and Transporter [45]. Finally, an ablation study shows that each constituent element of DiPac—learning, planning, and trajectory optimization—is essential for good performance.

One main limitation of our current work is particle state acquisition. We assume that a set of representative particles can be acquired from RGBD images of the object. This assumption may fail with complex objects or environments, e.g., cloth, because of occlusion or self-occlusion. Nevertheless, our evaluation tasks (Fig. 1) represent a substantial range of interesting objects that DiPac succeeds on.

II. RELATED WORKS

A. Model-based DOM

Model-based DOM methods have been studied widely [7, 25, 44]. They leverage a model that connects robot action with object deformation, allowing the robot to anticipate the object’s responses and choose the right action accordingly. The model may be manually designed [7, 44] or learned from data [13, 14, 22, 43, 39]. It may also adapt to real-world dynamics online [5, 40].

DiPac connects with the model-based approach. It uses a general-purpose particle dynamics simulator as the model, with the simulation model parameters learned from data. One key advantage of this model is a single, unified representation

for deformable objects of many different types, compared with existing methods that use object-specific representations. DiPac shares this underlying idea with earlier work [20], but combines planning, trajectory optimization, and learning to achieve much stronger results on a variety of deformable objects with a real robot.

B. Data-driven DOM

With the advances in machine learning, data-driven DOM methods are gaining success increasingly. Many of them learn robot actions directly from expert demonstrations [18, 23, 45, 34, 31]. Some learn a latent representation aimed at an object’s underlying physical properties, enabling the robot to reason about object behaviors in different scenarios [37, 10].

One highly successful example of data-driven DOM recently is Diffusion Policy [6], which sets a new benchmark for a broad the spectrum of manipulation tasks, including some DOM tasks.

Despite the success, data-driven methods often struggle with generalization to unseen scenarios, because of data scarcity, i.e., the difficulty of acquiring sufficient real-world robot demonstration data. DiPac tackles the difficulty by combining the strengths of data-driven and model-based approaches. The particle dynamics simulation model serves as a general physics prior for learning DOM tasks.

C. Differentiable Dynamics

Differentiable dynamics simulators, such as PlasticineLab [15], DiSECT [11], DiffSim [28], and DaxBench [3], offer a powerful tool for robot manipulation. They have two distinct uses. First, they may serve as a dynamics model in various simulation, control, and learning tasks [8, 32, 38]. Second, they provide a simulation environment for learning robot control policies [4, 9, 26, 42]. Our use in DiPac belongs to the former.

In both cases, a significant challenge is to bridge the gap between the simulated and real-world dynamics [1]. One general idea is to learn model parameters from real-world data [20, 24, 33]. DiPac follows this idea and calibrates the particle dynamics model, using data from a small number of interactions with the object in the real world. Compared with earlier work, DiPac has a distinct objective in model calibration: instead of uncovering the underlying physics, it aims to narrow the distance between the predicted and actual states in the *observation* space, for improved action selection.

III. PROBLEM FORMULATION

DiPac takes RGBD images of a deformable object as input and outputs a sequence of robot manipulation actions in task space, until a specified goal is reached.

We represent a deformable object as a set of *particles*. Each particle is a point of the object, with 3-D position, velocity, mass, as well as other attributes that characterize the interaction of this particle with other particles and the environment. The set of particles fully determines the *state* of the object. We measure the similarity between two states using

the Chamfer distance for shape matching over the positional components of the particles. Let P and Q be two point sets in 3-D. The Chamfer distance between P and Q is

$$\sigma(P, Q) = \frac{1}{|P|} \sum_{p \in P} \min_{q \in Q} \|p - q\|_2^2 + \frac{1}{|Q|} \sum_{q \in Q} \min_{p \in P} \|q - p\|_2^2.$$

We assume a differentiable simulator that captures the dynamics of the particle system:

$$x_{t+1} = f(x_t, u_t; \varphi),$$

where x_t and u_t are the particle state and the robot action at time t , respectively. The set φ contains the dynamics parameters describing, e.g., object rigidity, environment friction, etc.. The function f is differentiable with respect to x_t, u_t and φ . By default, we implement f using a recent *material point method* (MPM) [12, 36], but there are many alternatives (Section II). Details on MPM are available in Appendix A. DiPac is given an initial state x_0 and goal state x^g . It aims to find a sequence of actions (u_0, u_1, \dots) that minimize the total cost J over maximum T time steps:

$$J(x_0, U_{0:T-1}) = \sum_{t=0}^{T-1} c(x_t, u_t). \quad (1)$$

To reach the goal state x^g as closely as possible, we define the following cost function

$$c(x_t, u) = \sigma(x_t, x^g) - \sigma(x_{t-1}, x^g) + \zeta(x_t, u_t), \quad (2)$$

where the similarity to the goal state is measured using the Chamfer distance σ , and contact cost ζ is the L2 distance between the gripper and object.

Our premise in this work is that only a limited amount of real-world expert demonstration data, such as 10 episodes, is available from real robots. This constraint reflects the practical challenges of data collection, including the logistical difficulties, the time and effort required for gathering and annotating data, and the potential strain on robotic hardware. Given these challenges, our focus intensifies on creating learning algorithms that can leverage this sparse data effectively, underscoring the need for models that are data efficient.

IV. DEFORMABLE OBJECT MANIPULATION WITH DIFFERENTIABLE PARTICLES

A. Overview

DiPac presents a novel approach for manipulating deformable objects by integrating learning, planning, and differentiable trajectory optimization into a cohesive framework. Our approach operates in two phases: the learning phase, where model parameters are estimated to predict a better behavior of deformable objects for action selection, and the testing phase, which employs a guided differentiable planner to select optimal actions. Central to our approach is the unique combination of a tree-structured planning mechanism, guided by learned policies, with differentiable dynamics for action optimization along trajectories. This integration effectively addresses common challenges, such as poor initialization and

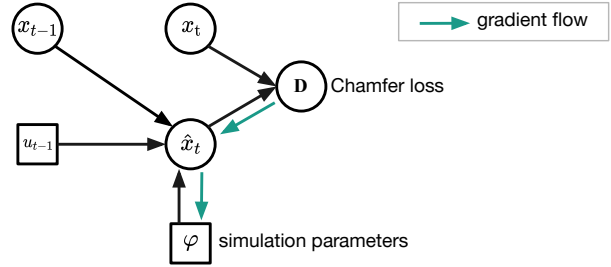


Fig. 2: Model calibration. The gradient-based optimization updates the parameter set φ to minimize the Chamfer distance between the predicted state \hat{x}_t and the observed particle state x_t .

local minima, by leveraging learned policy initialization and random policy branching. DiPac introduces a new perspective on policy formation, combining planning, learning, and differentiable optimization in a way that enhances both the efficiency and applicability of deformable object manipulation.

B. Particle State Construction

In this work, we assume there is no occlusion and reasonable object segmentation can be obtained from the top-down RGBD camera.

DiPac acquires the particle states by reconstructing them in real-time from multi-view RGBD images. We first extract the particles from the depth image to create a point cloud, then use a segmentation mask from the RGB images to eliminate background points and retain only the object-related points. For simplicity and speed, we use color filtering but it can be substituted with a more advanced segmentation technique, for example, Segment Any Thing [17, 29]. The final point cloud of the object is obtained by merging points from each view, and the unobserved interior is then filled with uniformly sampled particles to model the deformable object. When a depth camera is not available, multi-view RGB images can still be used to reconstruct the object shape for manipulation tasks [2].

The particle-based state representation allows us to predict the future states using the material point method (MPM) [12, 36]. In particular, the MPM simulation engine can roll out particle states to predict the next state $x_{t+1} = f(x_t, u_t; \varphi)$, resolving the long-standing challenge of lack of accurate dynamics models for deformable objects, enabling model-based planning and model predictive control methods to be applied to more complex manipulation tasks.

C. Dynamics Model Calibration

To enhance the accuracy of the simulator, we update the dynamics parameters, the object's stiffness and the friction coefficient, using a small amount of interaction data from the real robot. This calibration helps ensure that the actions optimized in the simulator produce similar results in the real world, essential for the successful deployment of DiPac in real-world applications. In detail, for each task, we collect 10 expert demonstrations from the real world via human teleoperation

with random initial positions and poses of the deformable object. Those expert demonstrations consist of RGBD images and expert actions for each step.

The differentiable particle representation enables direct optimization of the dynamics parameters through gradient descent. We illustrate this process in Fig. 2. A single trajectory consists of a sequence of observations $o_{0:T}$ and actions $u_{0:T-1}$ from the real world, then is converted into a particle state trajectory $x_{0:T}$. For each pair (x_t, u_t) in $(x_{0:T-1}, u_{0:T-1})$, our model predicts the next state $(\hat{x}_{1:T})$ in the simulation. To minimize the discrepancy between the simulation and the real world, we minimize the difference between the predicted states $(\hat{x}_{1:T})$ and the real states $(x_{1:T})$. As the particle-based transition function $f(x_t, u_t; \varphi)$ is differentiable, the dynamics parameters φ of the simulator can be optimized through gradient descent, using the following objective function:

$$\varphi = \arg \min_{\varphi} \sum_{t=0}^{T-1} \sigma(f(x_t, u_t; \varphi), x_{t+1}), \quad (3)$$

where $\sigma(\cdot, \cdot)$ is the Chamfer distance that measures the *unordered set* distance between the predicted particles \hat{x}_{t+1} and the observed particles x_{t+1} . In this way, we *do not require the particle correspondence* for calculating the Chamfer distance. Minimizing the distance of all transition pairs allows us to align our simulated dynamics model with the observed deformable object behaviors. Our purpose is for better action selection instead of creating a simulation that achieves the ground truth dynamics model.

D. Integrating Learning, Planning, and Optimization

With the learned dynamics model, we can search for the best actions. We introduce the Trajectory Tree Optimization algorithm to optimize trajectories sampled from a learned initial policy. This planner leverages differentiable trajectory optimization to achieve low sample complexity and efficient updates by pushing gradients directly. However, gradient-based methods can get stuck in local optima and are highly dependent on initial conditions [3]. To address these limitations, our planner uses a tree structure to select the best trajectory over multiple trajectories, initialized by randomly sampling a few initial actions (as depicted in Figure 3). This diversifies the initial states of the trajectories, helping to escape local optima and improve overall planning performance.

We implement our planner with a planning horizon H . Note that this planning horizon H is smaller than the task horizon T to save computation. At each time step $t = 0, \dots, T-1$, our planner plans a locally optimal trajectory with horizon H from the current initial state and executes the first planned action. It then repeats this process and re-plans at the next state until it exhausts the task horizon T .

We formalize the objective function for our trajectory tree optimization below. Given the current initial state x_0 and a sequence of actions $U_{0:H-1} = (u_0, u_1, \dots, u_{H-1})$ of length H , the total cost of the induced trajectory is the sum of the step-wise cost for each state-action pair. The objective function

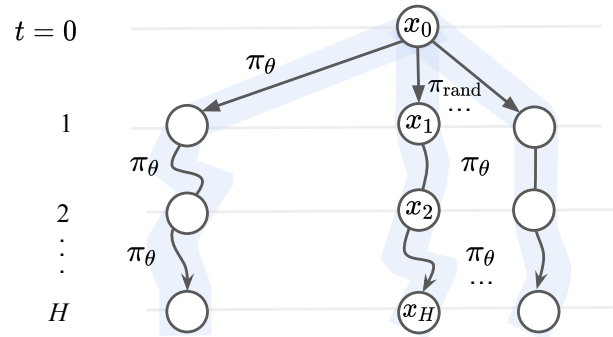


Fig. 3: Action selection via differentiable trajectory tree optimization. The search for the best action is guided by a learned initial policy π_θ , together with random exploration policy π_{rand} . After rollouts, DiPac minimizes the total trajectory cost by back-propagating the gradient along each sampled trajectory.

is to find the action sequence $U_{0:H-1}^*$ that minimizes this total cost:

$$U_{0:H-1}^* = \arg \min_{U_{0:H-1}} J(x_0, U_{0:H-1}) = \sum_{t=0}^{H-1} c(x_t, u_t), \quad (4)$$

whereas $x_{t+1} = f(x_t, u_t; \varphi)$ is given by transition function.

Our planner inherently supports close-loop planning: for each time step, after executing the first control from the optimized control sequence $U_{0:H-1}^*$, it will start re-planning at the new state.

Unlike standard trajectory optimization algorithms, our planner takes advantage of a learned initial policy to make the trajectory optimization more efficient. In particular, we use a learned policy to initialize the sampling distribution of the trajectory, increasing computational efficiency and reducing sample complexity. Directly optimizing the objective function in equation (4) is computationally intractable in the high-dimensional continuous state space. Even the naive Monte Carlo Tree Search in such a continuous action space requires a large amount of simulations for a good approximation. To make the optimization tractable, we use an initial policy to guide the trajectory rollouts and directly optimize the rollout trajectories through the gradients. A good policy can either initialize us with a near-optimal trajectory or enable us to optimize the gradients on a good optimization landscape. Either way, learning a good initial policy can help our planner to find the optimal solution more efficiently.

The trajectory tree, as shown in Figure 3, balances sample complexity, computation speed, and final performance. We first generate k random actions, $u_0^{1:k}$, by uniformly sampling a particle as the starting point and an angle to create a vector in a random direction to form the action. These actions are used for exploration. Additionally, we generate one action, u_0^0 , from an initial policy π_θ for exploitation. Next, we use π_θ to rollout for total H steps from all $u_0^{0:k}$.

We then use gradient descent to optimize the actions over each trajectory, where the objective function is the total cost of

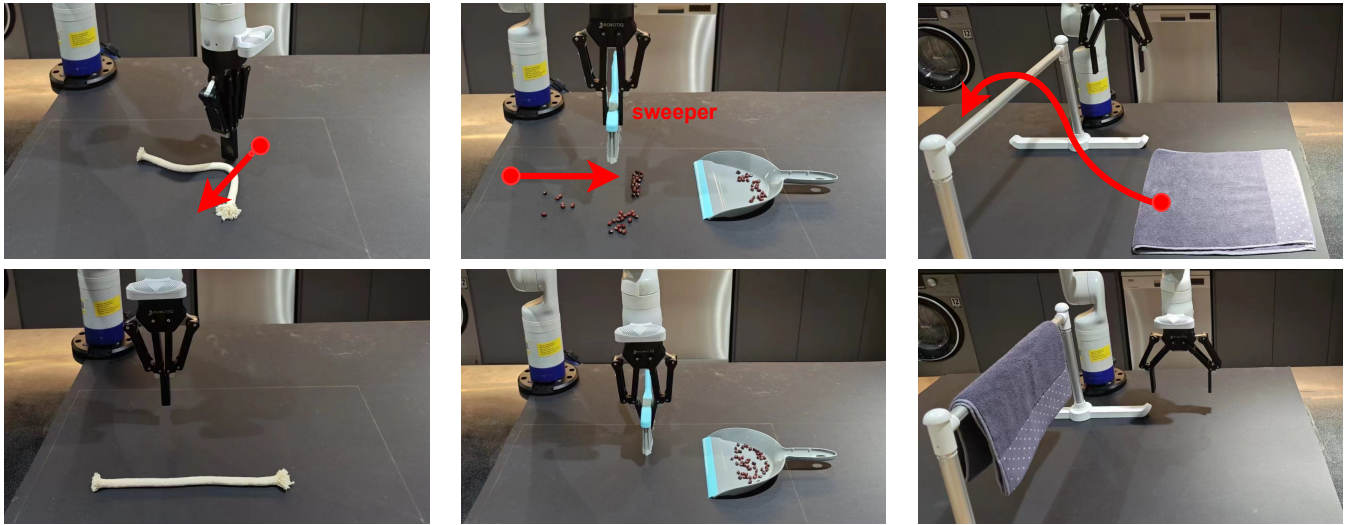


Fig. 4: Real-robot experiments setup. The top row shows robot actions. The bottom row shows the desired goal states.

the induced trajectory under the transition function $f(x, u, \varphi)$. The optimization is performed as follows:

$$u_t \leftarrow u_t - \eta \nabla_{u_t} J(x_t, U_{t:H-1}), \quad (5)$$

Where η is the learning rate. As the transition function and objective function are fully differentiable, we can update the actions by simply pushing the gradients. The total of $k + 1$ action candidates are optimized simultaneously and can be fully parallelized. The action that minimizes the objective function will be selected for real robot execution.

The differentiable trajectory tree optimization uses an initial policy to guide the search and approximate the objective function. DiPac’s initial policy uses Transporter [45], where images are rendered from particles as input and actions as output. DiPac is not limited to a specific choice of the initial policy. Alternatively, we can also use a Reinforcement Learning (RL) policy or a rule-based heuristic policy as the initial policy.

V. ROBOT EXPERIMENTS

We evaluated DiPac on three DOM tasks on a Kinova Gen3 robot (Fig. 1a–c). We further evaluated two liquid or liquid-solid pouring tasks in simulation (Fig. 1d–e), as it is difficult to carry out repeated pouring tasks on a real robot due to hardware limitations.

We summarize the experimental findings below:

- DiPac performs well on the spectrum of different deformable objects under evaluation: beans, rope, cloth, liquid, and liquid-solid mixture (Fig. 5 and Table I).
- DiPac outperforms a pure model-based planning method, CEM-MPC; it also outperforms two state-of-the-art data-driven learning methods, Diffusion Policy and Transporter (Fig. 5 and Table I).
- Initial policy learning, planning, and trajectory optimization each contributes strongly to the best online action selection (Fig. 6).

We first describe the tasks and the task-specific implementation details. The state space for all tasks is covered in Section III. For each task, the action space, and experiment setup are described below. Hyperparameters utilized by DiPac for each task are listed in Appendix Table II. We collect 10 expert demonstrations from the real world via human teleoperation for each task with random initial positions and poses. Those expert demonstrations, which consist of RGBD images and expert actions, are used in the training of initial policy and all the data-driven baseline methods, as well as learning model parameters.

A. Rope Pushing

The task is to push the rope to reach a target configuration (Fig. 4a).

a) Action Space: Each action is specified by the starting point for pushing, followed by a sequence of 20 displacements, i.e. $(x_0, y_0, \Delta x_0, \Delta y_0, \dots, \Delta x_{19}, \Delta y_{19})$, whereas x_0, y_0 specifies the start position of the gripper, and $\Delta x_i, \Delta y_i$ is the displacement for each sub-pushing action. The dimension of the action space is thus 42. Such a large action space enables flexible maneuver skills, for example, curved push to match a target curve shape.

b) Experiment Setup: We repeat the test 10 times with random starting positions and poses. The initial policy is obtained from an imitation learning method, Transporter [45] and the task horizon is 30. The desired goal state is extracted from an RGBD image and provided to all the methods.

B. Bean Sweeping

The task is to sweep beans into a tray (Fig. 4b).

a) Action Space: The action space is defined by the push-start point (x_0, y_0) and the push-end point (x_1, y_1) on the table. The dimension of the action space is 4.

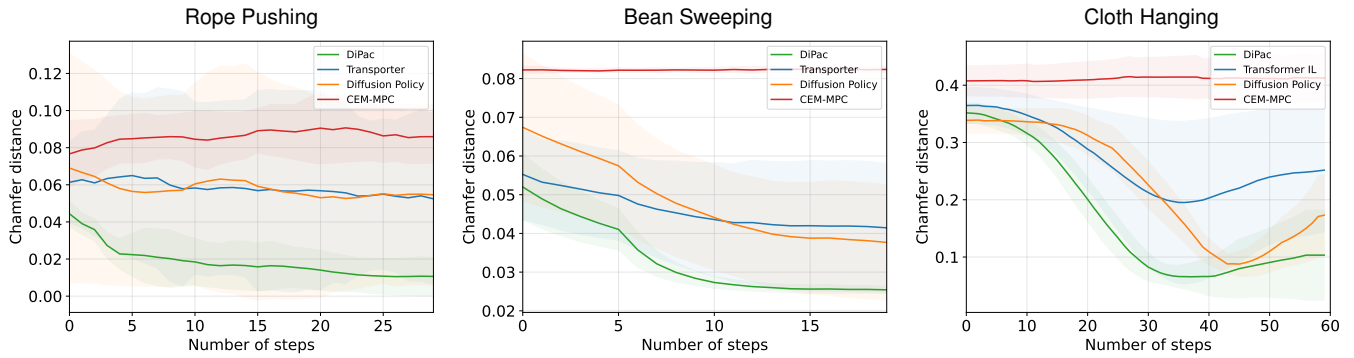


Fig. 5: Real robot deformable object manipulation task results on three different materials. We report the averaged Chamfer distance (meters) over steps.

b) Experiment Setup: The experiment setup is the same as the rope pushing task, except that the task horizon is 20. We use a fixed number of 50 red beans with random initial positions and configurations in the working space.

C. Cloth Hanging

This task involves the dexterous manipulation of a piece of cloth in a 3D space, aiming to accurately hang it on a designated rack. This sophisticated task encompasses various challenges, including the accurate control of the robot gripper to grasp, transport, and release the cloth at precise locations and orientations to ensure that it remains on the rack.

a) Action Space: The action space for this task is defined by a sequence of 8 small actions at each time step, with each action having a shape of $(8, 4)$. These actions represent the positions of the end-effector (robot gripper) in 3D space (3 dimensions for position and 1 dimension to signify the gripper’s state, open or closed). The decision to open or close the gripper is crucial, particularly when releasing the cloth over the rack.

b) Experiment Setup: The primary factor for success in this task is the stable placement of the cloth on the rack. A maximum task horizon of 60 steps is set to ensure efficiency in task completion while allowing sufficient flexibility for strategic maneuvering and adjustments. We assume the goal state is given and we evaluate 10 episodes for all methods with different starting positions and poses. A misjudgment of the release position can result in the cloth sliding off the rack and onto the table below, which results in increased distance to the goal state. For this 3D manipulation task, Transformer-based IL [46] has been used here for the initial policy.

D. Liquid and Soup Pouring

To further investigate the potential of DiPac, we conduct additional experiments that manipulate liquid in simulation. We use DaXBench [3] to simulate 2 robotic tasks: Pour Water and Pour Soup.

a) Action Space: The Pour Water task involves pouring water into a target bowl, using 6-D velocity and rotation controls in 100 steps. The Pour Soup task is similar but

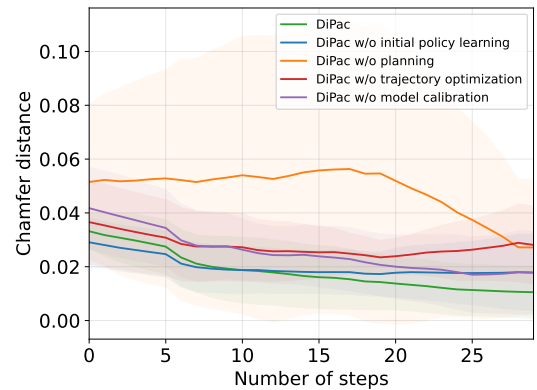


Fig. 6: Ablation study on rope pushing.

with solid ingredients, lasting 120 steps and using the same controls. The ground truth dynamics model is provided for all methods. These tasks present significant challenges as they require precise robot control of deformable objects, such as water, which are more difficult to manipulate due to their fluid and unpredictable nature. Achieving specific goals in a limited time frame is a major challenge in these tasks.

b) Baselines: We compare DiPac approach to Diffusion Policy, and baselines from the benchmark DaxBench [3] including ILD [4], a differentiable imitation learning method, as well as three variants of trajectory optimization methods that are classic non-differentiable Model Predictive Control and two differentiable implementations. Some data-driven methods, such as Transporter [45], are limited to pick-and-place actions and are therefore not applicable to the fine-grained action tasks we examine here.

E. Results

The results for the tasks of Rope Pushing, Bean Sweep, and Cloth Hanging, as depicted in Fig. 5. It underscores the superior performance of DiPac over established baselines, including Transporter [45], a data-driven method for deformable object manipulation; Diffusion Policy [6], a state-of-the-art method for object manipulations including deformable objects;

| Task | Planning | | | Ours | Imitation Learning | |
|------------|----------------------|-----------------------|---------------------------|--------------------|--------------------|------------------|
| | CEM-MPC [†] | Diff-MPC [†] | Diff-CEM-MPC [†] | DiPac | ILD [†] | Diffusion Policy |
| Pour-Water | 0.58±0.01 | 0.30±0.00 | 0.58±0.01 | 0.69 ± 0.01 | 0.32±0.03 | 0.66±0.17 |
| Pour-Soup | 0.56±0.01 | 0.44±0.00 | 0.55±0.02 | 0.76 ± 0.11 | 0.42±0.12 | 0.40±0.09 |

TABLE I: Simulation Results. Task performance is measured using the normalized reward. [†] We use numbers reported in the deformable object manipulation benchmark DaxBench [3]. More details of tasks can be found in Appendix section C. We report the mean and standard deviation evaluated with 20 seeds.

and CEM-MPC [30], a traditional non-differentiable trajectory optimization method.

DiPac significantly outperforms all baseline methods across the board. Its ability to efficiently handle complex, nonlinear dynamics and high degrees of freedom inherent in real robot deformable object manipulation tasks is clearly demonstrated. This is in stark contrast to the performance of the Diffusion Policy and Transporter methods, which exhibit considerable difficulties in adapting to unseen states during Bean Sweeping, Rope Pushing, and Cloth Hanging tasks. Although these imitation learning (IL) methods show competence in environments closely resembling their training demonstrations, their efficacy drops markedly in unfamiliar settings, leading to high variance in performance. This variance underscores the adaptability challenge that DiPac effectively overcomes, showcasing its robustness and the rapid convergence of its manipulation strategies.

In the task of Cloth Hanging, incorrect release positions result in the cloth slipping off onto the table, which is reflected in the end stages of the performance curve where the Chamfer distance tends to increase. This rise in the curve serves as an indicator of the manipulation policy’s effectiveness; the lesser the increase, the more capable the policy at managing such precise tasks. DiPac’s performance in this regard indicates its superior manipulation capabilities, further highlighting its advantage over the baselines.

The results for the tasks of Pour Water and Pour Soup are depicted in Table I. DiPac approach demonstrates superior performance compared to the baselines on the two liquid tasks. DiPac outperforms ILD by nearly double on the tasks of pouring water and soup. For the trajectory optimization methods, we improve performance consistently outperform these methods by a large margin on the two tasks. The manipulation of liquid to a specific configuration poses significant challenges in deformable object manipulation, resulting in high sample complexity and computation overhead for data-driven approaches and non-differentiable trajectory optimization. The results demonstrate that DiPac is a highly effective method for general DOM tasks, delivering promising performance compared to existing methods on these challenging DOM tasks.

In summary, DiPac not only surpasses its counterparts by a significant margin in all tasks but also demonstrates an exceptional ability to quickly and effectively converge to a good manipulation strategy. Its success in addressing the high variance seen in IL methods in unfamiliar scenarios and its

proficiency in executing tasks requiring high precision, emphasize its potential in real-world applications of deformable object manipulation.

F. Ablation Study

To highlight the individual components’ contributions of our combined planner with planning, learning, and differentiable optimization, we conducted an ablation study on the real robot manipulation task of pushing a rope. Especially, we aimed to elucidate the importance of i) incorporating a calibrated simulated dynamics model, ii) trajectory optimization based on differentiability, iii) exploration during the initial steps, and iv) having guidance from a learned IL policy. To do so, we incorporated these elements into four different systems and assessed them one by one.

- DiPac w/o model calibration: We eliminate the differentiable model calibration procedure and substitute it with a random selection for the dynamics parameters (both rigidity and ground friction).
- DiPac w/o trajectory optimization: In this model, we exclude the differentiable trajectory optimization from our proposed planner, but keep the model calibration.
- DiPac w/o planning: We omit the random exploration at the initial steps, and conduct the optimization purely on the only trajectory roll out from the initial policy.
- DiPac w/o initial policy learning: We do not use any initial policy, rather a random policy is used to guide the proposed planner.

Overall, each component is critical for effective task performance. The results of the ablation study confirm the significance of every individual component that constitutes our proposed planner. Without differentiable optimization or exploration, the performance suffers remarkably, pointing at these two elements being critical for trajectory optimization in deformable object manipulation. Also, unless the dynamics gap is reduced, a drop in task performance is observed. This supports our claim of the necessity of each individual component, thereby establishing the novelty of our ‘planning + learning + differentiable trajectory optimization’ approach. This unique assembly not only introduces a novel perspective on forming policy but also leverages the benefits of each component to master complex manipulation tasks efficiently.

G. Adaptation to New Dynamics

Moreover, DiPac can easily adapt to new dynamics. We use DiPac-Online, an extension of DiPac to adapt to sudden dynamics changes through online calibration. DiPac-Online

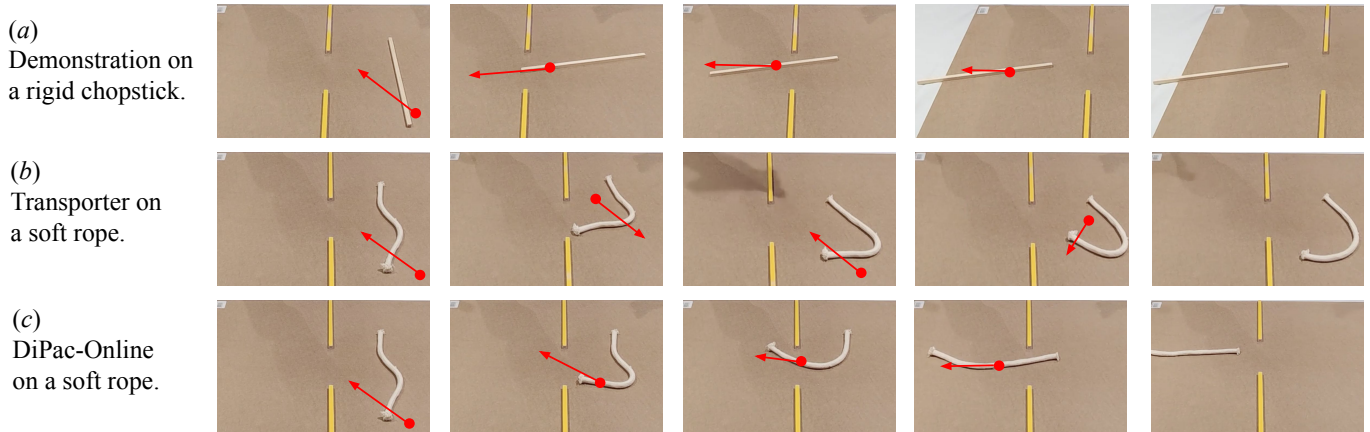


Fig. 7: Policy transfer to a new domain. The task is to push an object through a narrow gap between obstacles. (a) The expert demonstration pushes a rigid chopstick through by reorienting it. (b) Transporter tries to push through a soft rope but fails. (c) DiPac-Online succeeds, as it adapts to the changed dynamics by learning the dynamics parameters online.

was initially trained on a rigid-rod pushing task and then transferred to a soft-rope pushing task, which has vastly differing dynamics. The video can be viewed in the supplementary files. Using the Transporter [45] and DiPac methods, we set out to complete the task of pushing a rigid rod and soft rope through a small opening to the left area, shown in Fig. 7. We start by collecting 10 expert demonstrations on the rigid rod to train both the Transporter and DiPac’s initial policy. However, when the Transporter is transferred to roll out on the soft rope, it fails to complete the task due to the deformation of the rope which created states unseen in the training distribution. In contrast, DiPac is successful in completing the task, by continuously estimating the simulation parameters and calibrating the dynamics on the fly. DiPac can leverage the deformation of the rope and utilize planning to complete the task. This demonstrates the effectiveness of DiPac in tackling dynamics transfer scenarios.

VI. DISCUSSION

DiPac has achieved impressive outcomes in manipulating a variety of deformable objects, such as rope, cloth, beans and liquid. This is possible due to its utilization of the particle representation, which is flexible and expressive enough to universally describe the underlying states of all deformable objects. Additionally, DiPac takes advantage of the recent improvement of differentiable dynamics simulators, enabling the sampled trajectories to be optimized through back-propagation, thus improving its computation speed and reducing the sample complexity of trajectory optimization.

Our current assumption is that there is no occlusion in the multi-view RGBD images. This allows us to directly extract the particle states from the segmentation masks of the deformable objects. However, this simplifying assumption could limit the performance of DiPac in more complex environments, where factors such as occlusions, motion blur, and background clutter make extracting the particle information challenging. Therefore, our next step is to develop a more robust and

efficient algorithm for particle extraction, allowing us to apply DiPac to unstructured and more complex environments.

We would like to scale DiPac to tasks with more complex optimization landscapes in the future. However, more challenging tasks with multiple local optima and non-smooth/discontinuous landscapes may require careful design of the gradient-based optimization algorithms to handle such scenarios. We conjecture that our initial policy guidance can be useful in cases, where a good initialization of the landscape can significantly reduce the computational cost of gradient-based optimization. This approach is analogous to AlphaGo [35]: both use a pre-learned policy or a value function to estimate the future returns of the current action, allowing for a shorter search depth without compromising much on the optimality. We intend to better understand the impact of initial policies and the optimization process on the overall system performance.

VII. CONCLUSION

In conclusion, we present DiPac, a general algorithm that enables manipulation of a wide range of deformable objects using differentiable dynamics in simulation and on real robots. DiPac represents deformable objects as differentiable particles, which helps to reduce the gap between simulation and reality. DiPac also provides a new perspective on how policy can be formed, by combining learning, planning, and differentiable trajectory optimization. The experiments demonstrate DiPac’s ability to effectively perform diverse tasks, such as rope pushing, bean sweeping, and cloth hanging. Additionally, DiPac demonstrates exceptional transferability, addressing a current challenge in the understanding of deformable objects. Looking ahead, it will be crucial and valuable to explore the application of DiPac to more complex and diverse tasks, as well as to extend the method to handle objects with more intricate dynamics.

REFERENCES

- [1] Yevgen Chebotar, Ankur Handa, Viktor Makoviychuk, Miles Macklin, Jan Issac, Nathan Ratliff, and Dieter Fox. Closing the sim-to-real loop: Adapting simulation randomization with real world experience. In *2019 International Conference on Robotics and Automation (ICRA)*, pages 8973–8979. IEEE, 2019.
- [2] Siwei Chen, Xiao Ma, Yunfan Lu, and David Hsu. Ab Initio Particle-based Object Manipulation. In *Proceedings of Robotics: Science and Systems*, July 2021. doi: 10.15607/RSS.2021.XVII.071.
- [3] Siwei Chen, Yiqing Xu, Cunjun Yu, Linfeng Li, Xiao Ma, Zhongwen Xu, and David Hsu. Daxbench: Benchmarking deformable object manipulation with differentiable physics. In *The Eleventh International Conference on Learning Representations*, 2022.
- [4] Siwei Chen, Xiao Ma, and Zhongwen Xu. Imitation learning as state matching via differentiable physics. In *Proceedings of the IEEE/CVF Conference on Computer Vision and Pattern Recognition*, pages 7846–7855, 2023.
- [5] Cheng Chi, Benjamin Burchfiel, Eric Cousineau, Siyuan Feng, and Shuran Song. Iterative residual policy for goal-conditioned dynamic manipulation of deformable objects. In *Proceedings of Robotics: Science and Systems (RSS)*, 2022.
- [6] Cheng Chi, Siyuan Feng, Yilun Du, Zhenjia Xu, Eric Cousineau, Benjamin Burchfiel, and Shuran Song. Diffusion policy: Visuomotor policy learning via action diffusion. In *Proceedings of Robotics: Science and Systems (RSS)*, 2023.
- [7] Marco Cusumano-Towner, Arjun Singh, Stephen Miller, James F O’Brien, and Pieter Abbeel. Bringing clothing into desired configurations with limited perception. In *2011 IEEE international conference on robotics and automation*, pages 3893–3900. IEEE, 2011.
- [8] Filipe de Avila Belbute-Peres, Kevin Smith, Kelsey Allen, Josh Tenenbaum, and J. Zico Kolter. End-to-end differentiable physics for learning and control. In S. Bengio, H. Wallach, H. Larochelle, K. Grauman, N. Cesa-Bianchi, and R. Garnett, editors, *Advances in Neural Information Processing Systems*, volume 31. Curran Associates, Inc., 2018.
- [9] C Daniel Freeman, Erik Frey, Anton Raichuk, Sertan Girgin, Igor Mordatch, and Olivier Bachem. Brax—a differentiable physics engine for large scale rigid body simulation. *arXiv preprint arXiv:2106.13281*, 2021.
- [10] Aditya Ganapathi, Priya Sundaesan, Brijen Thananjeyan, Ashwin Balakrishna, Daniel Seita, Jennifer Grannen, Minh Hwang, Ryan Hoque, Joseph E Gonzalez, Nawid Jamali, et al. Learning dense visual correspondences in simulation to smooth and fold real fabrics. In *2021 IEEE International Conference on Robotics and Automation (ICRA)*, pages 11515–11522. IEEE, 2021.
- [11] Eric Heiden, Miles Macklin, Yashraj Narang, Dieter Fox, Animesh Garg, and Fabio Ramos. Disect: A differentiable simulation engine for autonomous robotic cutting. *arXiv preprint arXiv:2105.12244*, 2021.
- [12] Yuanming Hu, Yu Fang, Ziheng Ge, Ziyin Qu, Yixin Zhu, Andre Pradhana, and Chenfanfu Jiang. A moving least squares material point method with displacement discontinuity and two-way rigid body coupling. *ACM Transactions on Graphics (TOG)*, 37(4):1–14, 2018.
- [13] Zhe Hu, Peigen Sun, and Jia Pan. Three-dimensional deformable object manipulation using fast online gaussian process regression. *IEEE Robotics and Automation Letters*, 3(2):979–986, 2018.
- [14] Zhe Hu, Tao Han, Peigen Sun, Jia Pan, and Dinesh Manocha. 3-d deformable object manipulation using deep neural networks. *IEEE Robotics and Automation Letters*, 4(4):4255–4261, 2019.
- [15] Zhiao Huang, Yuanming Hu, Tao Du, Siyuan Zhou, Hao Su, Joshua B Tenenbaum, and Chuang Gan. Plasticinlab: A soft-body manipulation benchmark with differentiable physics. *arXiv preprint arXiv:2104.03311*, 2021.
- [16] Peter Karkus, Xiao Ma, David Hsu, Leslie Pack Kaelbling, Wee Sun Lee, and Tomás Lozano-Pérez. Differentiable algorithm networks for composable robot learning. In *Proceedings of Robotics: Science and Systems (RSS)*, 2019.
- [17] Alexander Kirillov, Eric Mintun, Nikhila Ravi, Hanzi Mao, Chloe Rolland, Laura Gustafson, Tete Xiao, Spencer Whitehead, Alexander C. Berg, Wan-Yen Lo, Piotr Dollár, and Ross Girshick. Segment anything. *arXiv:2304.02643*, 2023.
- [18] Alex X Lee, Henry Lu, Abhishek Gupta, Sergey Levine, and Pieter Abbeel. Learning force-based manipulation of deformable objects from multiple demonstrations. In *2015 IEEE International Conference on Robotics and Automation (ICRA)*, pages 177–184. IEEE, 2015.
- [19] Jeong Hun Lee, Mike Y Michelis, Robert Katzschmann, and Zachary Manchester. Aquarium: A fully differentiable fluid-structure interaction solver for robotics applications. *arXiv preprint arXiv:2301.07028*, 2023.
- [20] Yunzhu Li, Jiajun Wu, Russ Tedrake, Joshua B Tenenbaum, and Antonio Torralba. Learning particle dynamics for manipulating rigid bodies, deformable objects, and fluids. *arXiv preprint arXiv:1810.01566*, 2018.
- [21] Xingyu Lin, Yufei Wang, and David Held. Learning visible connectivity dynamics for cloth smoothing. *arXiv preprint arXiv:2105.10389*, 2021.
- [22] Xingyu Lin, Yufei Wang, Zixuan Huang, and David Held. Learning visible connectivity dynamics for cloth smoothing. In *Conference on Robot Learning*, pages 256–266. PMLR, 2022.
- [23] Wen Hao Lui and Ashutosh Saxena. Tangled: Learning to untangle ropes with rgb-d perception. In *2013 IEEE/RSJ International Conference on Intelligent Robots and Systems*, pages 837–844. IEEE, 2013.
- [24] Peter Mitrano, Alex LaGrassa, Oliver Kroemer, and Dmitry Berenson. Focused adaptation of dynamics mod-

- els for deformable object manipulation. In *2023 IEEE International Conference on Robotics and Automation (ICRA)*, pages 5931–5937. IEEE, 2023.
- [25] Pol Monsó, Guillem Alenyà, and Carme Torras. Pomdp approach to robotized clothes separation. In *2012 IEEE/RSJ International Conference on Intelligent Robots and Systems*, pages 1324–1329. IEEE, 2012.
- [26] Miguel Angel Zamora Mora, Momchil Peychev, Sehoon Ha, Martin Vechev, and Stelian Coros. Pods: Policy optimization via differentiable simulation. In *International Conference on Machine Learning*, pages 7805–7817. PMLR, 2021.
- [27] Ashvin Nair, Dian Chen, Pulkit Agrawal, Phillip Isola, Pieter Abbeel, Jitendra Malik, and Sergey Levine. Combining self-supervised learning and imitation for vision-based rope manipulation. In *2017 IEEE international conference on robotics and automation (ICRA)*, pages 2146–2153. IEEE, 2017.
- [28] Yi-Ling Qiao, Junbang Liang, Vladlen Koltun, and Ming C Lin. Scalable differentiable physics for learning and control. *arXiv preprint arXiv:2007.02168*, 2020.
- [29] Xuebin Qin, Zichen Zhang, Chenyang Huang, Masood Dehghan, Osmar Zaiane, and Martin Jagersand. U2-net: Going deeper with nested u-structure for salient object detection. In *Pattern Recognition*, volume 106, page 107404, 2020.
- [30] Arthur George Richards. *Robust constrained model predictive control*. PhD thesis, Massachusetts Institute of Technology, 2005.
- [31] Gautam Salhotra, I-Chun Arthur Liu, Marcus Dominguez-Kuhne, and Gaurav S Sukhatme. Learning deformable object manipulation from expert demonstrations. *IEEE Robotics and Automation Letters*, 7(4):8775–8782, 2022.
- [32] C. Schenck and D. Fox. Spnets: Differentiable fluid dynamics for deep neural networks. In *Proceedings of the Second Conference on Robot Learning (CoRL)*, Zurich, Switzerland, 2018.
- [33] Connor Schenck and Dieter Fox. Spnets: Differentiable fluid dynamics for deep neural networks. In *Conference on Robot Learning*, pages 317–335. PMLR, 2018.
- [34] Daniel Seita, Pete Florence, Jonathan Tompson, Erwin Coumans, Vikas Sindhwani, Ken Goldberg, and Andy Zeng. Learning to rearrange deformable cables, fabrics, and bags with goal-conditioned transporter networks. In *2021 IEEE International Conference on Robotics and Automation (ICRA)*, pages 4568–4575. IEEE, 2021.
- [35] David Silver, Aja Huang, Chris J Maddison, Arthur Guez, Laurent Sifre, George Van Den Driessche, Julian Schrittwieser, Ioannis Antonoglou, Veda Panneershelvam, Marc Lanctot, et al. Mastering the game of go with deep neural networks and tree search. *nature*, 529(7587):484–489, 2016.
- [36] Deborah Sulsky, Zhen Chen, and Howard L Schreyer. A particle method for history-dependent materials. *Computer methods in applied mechanics and engineering*, 118(1-2):179–196, 1994.
- [37] Priya Sundareshan, Jennifer Grannen, Brijen Thananjeyan, Ashwin Balakrishna, Michael Laskey, Kevin Stone, Joseph E Gonzalez, and Ken Goldberg. Learning rope manipulation policies using dense object descriptors trained on synthetic depth data. In *2020 IEEE International Conference on Robotics and Automation (ICRA)*, pages 9411–9418. IEEE, 2020.
- [38] Marc Toussaint, Kelsey R. Allen, Kevin A. Smith, and Joshua B. Tenenbaum. Differentiable physics and stable modes for tool-use and manipulation planning. In *Robotics: Science and Systems*, 2018.
- [39] Angelina Wang, Thanard Kurutach, Kara Liu, Pieter Abbeel, and Aviv Tamar. Learning robotic manipulation through visual planning and acting. *arXiv preprint arXiv:1905.04411*, 2019.
- [40] Yixuan Wang, Yunzhu Li, Katherine Driggs-Campbell, Li Fei-Fei, and Jiajun Wu. Dynamic-Resolution Model Learning for Object Pile Manipulation. In *Proceedings of Robotics: Science and Systems*, Daegu, Republic of Korea, July 2023. doi: 10.15607/RSS.2023.XIX.047.
- [41] Zhou Xian, Bo Zhu, Zhenjia Xu, Hsiao-Yu Tung, Antonio Torralba, Katerina Fragkiadaki, and Chuang Gan. Fluidlab: A differentiable environment for benchmarking complex fluid manipulation. *arXiv preprint arXiv:2303.02346*, 2023.
- [42] Jie Xu, Viktor Makoviychuk, Yashraj Narang, Fabio Ramos, Wojciech Matusik, Animesh Garg, and Miles Macklin. Accelerated policy learning with parallel differentiable simulation. *arXiv arXiv:2204.07137*, 2022.
- [43] Wilson Yan, Ashwin Vangipuram, Pieter Abbeel, and Lerrel Pinto. Learning predictive representations for deformable objects using contrastive estimation. In *Conference on Robot Learning*, pages 564–574. PMLR, 2021.
- [44] Lazher Zaidi, Juan Antonio Corrales, Belhassen Chedli Bouzgarrou, Youcef Mezouar, and Laurent Sabourin. Model-based strategy for grasping 3d deformable objects using a multi-fingered robotic hand. *Robotics and Autonomous Systems*, 95:196–206, 2017.
- [45] Andy Zeng, Pete Florence, Jonathan Tompson, Stefan Welker, Jonathan Chien, Maria Attarian, Travis Armstrong, Ivan Krasin, Dan Duong, Vikas Sindhwani, et al. Transporter networks: Rearranging the visual world for robotic manipulation. *arXiv preprint arXiv:2010.14406*, 2020.
- [46] Tony Z Zhao, Vikash Kumar, Sergey Levine, and Chelsea Finn. Learning fine-grained bimanual manipulation with low-cost hardware. In *Proceedings of Robotics: Science and Systems (RSS)*, 2023.

APPENDIX

A. Dynamics Transition Function

The state-of-the-art deformable objects simulators such as PlasticineLab [15] and DaXBench [3] utilize the MLS-MPM [12] method. In a nutshell, the MLS-MPM consists of three main steps:

Particle to Grid (P2G). In the process of P2G, the MLS-MPM first updates its deformation gradient \mathbf{F}_p^{n+1} given the previous \mathbf{F}_p^n and velocity gradient \mathbf{C}_p^n . It then computes the affine velocity \mathbf{A}_p^n to update grid velocity \mathbf{v} as shown below:

$$\begin{aligned}\mathbf{F}_p^{n+1} &= (\mathbf{I} + \Delta t \mathbf{C}_p^n) \mathbf{F}_p^n \\ \mathbf{A}_p^n &= m_p \mathbf{C}_p^n - \frac{4\Delta t}{\Delta x^2} \sum_p V_p^0 \mathbf{P}(\mathbf{F}_p^{n+1}) (\mathbf{F}_p^{n+1})^T \\ (m\mathbf{v})_i^{n+1} &= \sum_p w_{ip} \{m_p \mathbf{v}_p^n + \mathbf{A}_p^n (\mathbf{x}_i - \mathbf{x}_p^n)\}.\end{aligned}$$

We denote i as the grid index, p as the particle index, and n as the number of updates. The \mathbf{P} involves object properties such as rigidity to affect the deformation process. MLS-MPM aggregates the velocities of all the particles into a grid, which enables modeling the interactions among all particles without the need to search for neighbors of each individual particle.

Grid Operation (GO). The MLS-MPM then normalizes the grid velocity and computes boundary conditions (BC) as below:

$$\begin{aligned}\hat{\mathbf{v}}_i^{n+1} &= (m\mathbf{v})_i^{n+1} / m_i^{n+1} \\ \mathbf{v}_i^{n+1} &= \text{BC}(\hat{\mathbf{v}}_i^{n+1}).\end{aligned}$$

Grid to Particle (G2P). Finally, The MLS-MPM aggregates the velocity \mathbf{v} from grids and converts it back to particles. It then updates the velocity gradient \mathbf{C} and position \mathbf{x} :

$$\begin{aligned}\mathbf{v}_p^{n+1} &= \sum_i w_{ip} \mathbf{v}_i^{n+1} \\ \mathbf{C}_p^{n+1} &= \frac{4}{\Delta x^2} \sum_i w_{ip} \mathbf{v}_i^{n+1} (\mathbf{x}_i - \mathbf{x}_p^n)^T \\ \mathbf{x}_p^{n+1} &= \mathbf{x}_p^n + \Delta t \mathbf{v}_p^{n+1}.\end{aligned}$$

More details can be found in the MLS-MPM paper [12].

B. Implementation Details

There are 5 tasks studied in this work. For Rope Pushing and Bean Sweeping, PlasticineLab [15] is used as the differentiable simulation engine. For Cloth Hanging, Water Pouring and Soup Pouring, DaxBench [3] is used as the differentiable simulation engine. Both of them implement MLS-MPM as an underlying physics engine.

Visualizations We provide visualizations of particles rendered in simulation based on real-world observations in Fig. 8.

Hyper-parameters Table II shows the hyperparameters used in our real robot experiments for rope pushing, bean sweeping and t-shirt folding.

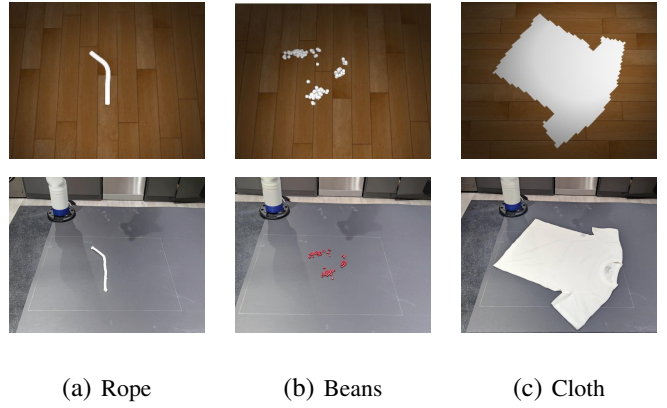


Fig. 8: Visualization. Bottom: deformable objects in the real world. Top: particle states rendered in simulation for different types of deformable objects.

TABLE II: Hyperparameters for DiPac on the real robot tasks

| Task | $k + 1$ | # GPUs | # Demos | Search Depth | # Particles |
|---------------|---------|--------|---------|--------------|-------------|
| Rope Pushing | 15 + 1 | 15 | 10 | 3 | 2000 |
| Bean Sweeping | 149 + 1 | 15 | 10 | 1 | 300 |
| Cloth Hanging | 15 + 1 | 4 | 10 | 3 | 1000 |

Computation Time Table III and Table IV show the computation time for each method and for each task. For model parameters learning, each gradient update takes about 20 - 40 seconds depending on the demonstrated trajectory length.

TABLE III: Computation time on the real robot tasks

| Method | Rope Pushing | Bean Sweeping | Cloth Hanging |
|------------------|--------------|---------------|---------------|
| Transporter | 2s | 2s | NA |
| Diffusion Policy | 1s | 1s | 1s |
| CEM-MPC | 90s | 90s | 60s |
| Dipac | 10s | 10s | 4s |

TABLE IV: Detailed Computation Time

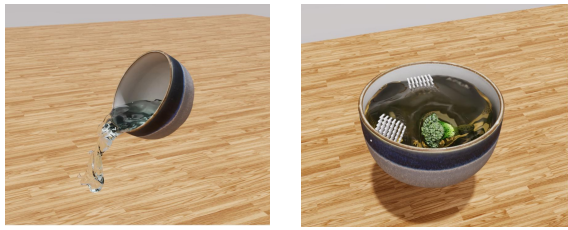
| Method | Rope Pushing | Bean Sweeping | Cloth Hanging |
|-------------------|--------------|---------------|---------------|
| Step Forward | 0.05s | 0.05s | 0.03s |
| Step Backward | 0.2s | 0.2s | 0.1s |
| Traj Optimization | 0.6s | 0.4s | 0.3s |

Interaction between end-effector and particles The two gripper fingers are simulated as two boxes in the simulation. Collision between particles and boxes are well captured in the physics engine.

C. Simulation Tasks

We present a comprehensive examination of simulations performed using the DaXBench platform [3]. The experiments encompass three distinct tasks, each with its own unique set of challenges and objectives.

Pour Water The Pour Water task requires the robot to pour a bowl of water into a target bowl, using control of velocity and



(a) Pour water[†]

(b) Pour Soup[†]

Fig. 9: We illustrate different deformable object manipulation tasks in simulation. [†] We use the example images from DaxBench [3].

rotation in Cartesian space. The robot holds the bowl and the action space is defined as a 6-dimensional vector, representing linear velocity along the x , y , and z axes, as well as angular velocity along 3 axes. The task is designed to last for 100 steps.

Pour Soup The Pour Soup task is similar in concept to the Pour Water task, but with the added challenge of solid ingredients mixed in with the water. These ingredients create additional interactions between the liquid and solid components, potentially leading to spills. As with the Pour Water task, the action space is defined as a 6-dimensional vector, with the same linear and angular velocity controls. The task horizon is set at 120 steps.

Each of these tasks offers a unique set of challenges and objectives. Since Transporter is not designed for low-level control tasks, we compare DiPac with four baselines in DaXBench, namely, ILD [4], CEM-MPC, Diff-MPC, Diff-CEM-MPC.

ILD is the latest differentiable-physics-based IL method; it utilizes the simulation gradients to reduce the required number of expert demonstrations and to improve performance.

Diff-MPC and Diff-CEM-MPC are two variants of Model Predictive Control that incorporate differentiable dynamics. Both methods optimize immediate rewards for each action using differentiable physics but differ in their initialization of action sequences. Diff-MPC starts with a random sequence, while Diff-CEM-MPC utilizes a sequence optimized by Cross-Entropy Method MPC (CEM-MPC).

DiPac uses a behavior cloning policy, with an image as input and action as output, as its initial policy. We use 1 GPU, 10 demonstrations for training initial policy, and search depths of the whole trajectory, 100, 120, and 70 for the 3 tasks. We outperformed all the baselines, demonstrating the effectiveness of our method.